Clays and Clay Minerals, Vol. 57, No. 2, 227–233, 2009.

POLARIZED ATR-FTIR INVESTIGATION OF Fe REDUCTION IN THE ULEY NONTRONITES

BRYAN R. BZDEK AND MOLLY M. MCGUIRE*
Department of Chemistry, Bucknell University, Lewisburg, PA 17837, USA

Abstract—Reduction of structural Fe in smectites affects the surface chemical behavior of the clay, but the underlying mechanism and changes in clay structure are still in need of investigation, particularly with respect to changes in the tetrahedral sheet. The purpose of this study was to probe changes in the tetrahedral sheet that occur when structural Fe is reduced in the Uley nontronites, NAu-1 and NAu-2, using polarized attenuated total internal reflection Fourier-transform infrared spectroscopy. Despite the differences in their structures – NAu-2 has tetrahedral Fe^{3+} while NAu-1 does not – the changes observed in the Si–O stretching region were quite similar. Reduction results in a shift of the in-plane Si–O stretching modes to lower frequencies, while the out-of-plane Si–O stretch shifts to higher frequencies. The magnitude of these shifts is greater in NAu-2 than in NAu-1, but the crystallinity of the tetrahedral silicate sheet of NAu-2 is preserved upon reduction. In both nontronites, the orientation of the out-of-plane Si–O bond changes and becomes completely perpendicular to the basal (001) surface of the clay, indicating the formation of trioctahedral domains wherein the individual tetrahedra reorient relative to the plane of the clay layer.

Key Words—ATR-FTIR, Infrared Spectroscopy, NAu-1, NAu-2, Nontronite, Reduction.

INTRODUCTION

The reduction of Fe^{3+} within the structure of nontronites and ferruginous smectites is a subject of interest due to the role of Fe-bearing clays in geochemical redox cycles and in particular the reductive degradation of common groundwater contaminants (*e.g.* Hofstetter *et al.*, 2006; Elsner *et al.*, 2004; Ribeiro *et al.*, 2004b; Cervini-Silva *et al.*, 2000, 2003; Nzengung *et al.*, 2001; Xu *et al.*, 2001; Yan and Bailey, 2001). A range of techniques including Mössbauer (Jaisi *et al*., 2005; Ribeiro *et al.*, 2004a; Komadel *et al.*, 1995), extended X-ray absorption fine structure (EXAFS) (Manceau *et al.*, 2000), and infrared (IR) (Lee *et al.*, 2006; Fialips *et al.*, 2002a, 2002b; Manceau *et al.*, 2000; Yan and Stucki, 1999, 2000; Komadel *et al.*, 1995; Stucki and Roth, 1976) spectroscopies has been used to investigate the reduction mechanism in these clays. Some details of the structural changes in the octahedral sheet accompanying reduction have been discerned: dehydroxylation of the octahedral sheet occurs (Drits and Manceau, 2000; Manceau *et al.*, 2000; Komadel *et al.*, 1995), as well as migration of the newly created Fe^{2+} from *cis*-octahedral to *trans*-octahedral sites (Manceau *et al.*, 2000). Furthermore, structural rearrangement results in the creation of trioctahedral domains within the originally dioctahedral structure (Manceau *et al.*, 2000).

As described above, the mechanism of Fe reduction in nontronites is focused predominantly on changes to the octahedral sheet. Such significant changes in structure, however, must also affect the adjoined tetrahedral sheets. Indeed, several IR spectroscopy studies have shown that the Si–O stretching bands shift by tens of wavenumbers upon reduction of structural Fe in nontronite (Fialips *et al.*, 2002b; Stucki and Roth, 1976) and ferruginous smectite (Fialips *et al.*, 2002a). More specifically, Yan and Stucki (1999) showed that the out-of-plane component of the Si–O stretching region shifts to higher frequency upon reduction of Fe^{3+} in montmorillonite, while the in-plane components shift to lower frequencies. These previous studies clearly indicate substantial structural modification to the tetrahedral sheet, but the details of this transformation remain to be determined. In this study, polarized infrared spectra of oriented nontronite films are presented in order to examine bond orientation changes that occur with reduction and further clarify the nature of the changes to the tetrahedral sheet. In a previous study, the O–H stretch of reduced nontronite was shown to exhibit pleochroic behavior after reduction of structural Fe (Fialips *et al.*, 2002b), but to date, no polarized infrared studies of the Si–O stretching region of reduced Fe-bearing clays have been presented in the literature.

The second purpose of this work was to examine the effect of the reduction of tetrahedral Fe^{3+} on the structure of the tetrahedral sheet. The Uley nontronites, NAu-1 and NAu-2, examined in this study were chosen to allow a comparison between a clay with only octahedral Fe^{3+} and one with both octahedral and tetrahedral Fe^{3+}. NAu-1 is a bright yellowish-green clay with structural formula

* E-mail address of corresponding author:
mmcguire@bucknell.edu
DOI: 10.1346/CCMN.2009.0570209

$M^{+}_{1.05}[Si_{6.98}Al_{1.02}][Al_{0.29}Fe_{3.68}Mg_{0.04}]O_{20}(OH)_4$ (Keeling *et al.*, 2000). Chemical and spectroscopic analyses of NAu-1 (Jaisi *et al.*, 2005; Gates *et al.*, 2002; Keeling *et al.*, 2000) have indicated that Fe^{3+}, as in most nontronites, is mainly located in the octahedral sheet. NAu-2 is a dark brown clay with the structural formula $M^{+}_{0.72}[Si_{7.55}Al_{0.16}Fe_{0.29}][Al_{0.34}Fe_{3.54}Mg_{0.05}]O_{20}(OH)_4$ (Keeling *et al.*, 2000) with ~8% of its Fe in tetrahedral coordination (Gates *et al.*, 2002). A comparison of these two clays will therefore allow a determination of the role of tetrahedral Fe^{3+} in the evolution of the silicate structure during reduction.

Infrared spectroscopy has been applied to the study of clay mineral structures using a variety of sampling techniques. Absorption studies in both transmission and reflectance modes (Madejová, 2003) as well as IR emission spectroscopy (Kloprogge and Frost, 2005) have been reviewed previously. The IR absorption data presented here were acquired using attenuated total reflection (ATR), which has several distinct advantages over other sampling techniques. Most importantly for this study, ATR allows for the characterization of an aqueous suspension *in situ* without additional sample preparation. In this technique, the IR beam is internally reflected within a crystal with a high refractive index. At each reflection point, an exponentially decaying evanescent wave escapes from the internal reflection element (IRE), allowing an absorption spectrum of any material in direct contact with the IRE to be acquired. The small effective penetration depth (~1 μm) of the evanescent wave allows an aqueous sample to be analyzed despite the strong absorption of water, making ATR ideal for *in situ* studies. Additionally, a suspension of clay particles forms a thin, oriented film on the IRE with the basal surfaces of the clay platelets parallel to the IRE surface (Johnston and Premachandra, 2001). In the present study, oriented films were examined with plane-polarized incident radiation in order to observe changes in bond orientation accompanying reduction of structural Fe.

MATERIALS AND METHODS

Clay preparation

The nontronites used in this study, NAu-1 and NAu-2 (Keeling *et al.*, 2000), were obtained from the Source Clays Repository of The Clay Minerals Society (www.clays.org/sourceclays/SourceClays.html). The clay was purified through a wet sedimentation process (Vaniman, 2001) in order to isolate the 0.35−2 μm size fraction of the mineral. Once the appropriate size fraction was collected, the clay was acid washed with 0.1 M acetic acid (Baker) to eliminate carbonate impurities. The clay was then rinsed three times with 18 MΩ-cm deionized water. Finally, Na^{+}-saturated samples were produced by washing the clay with 0.1 M NaCl (Fisher), followed by three washes with 18 MΩ-cm deionized water.

Structural Fe reduction

All chemical manipulations were performed in an anaerobic glovebox under an atmosphere of 95:5 N_2:H_2. A measured amount of sample (~30 mg) was dispersed in 20 mL of N_2-sparged 18 MΩ-cm deionized water. To this was added ~10 mL of N_2-sparged sodium citrate-bicarbonate buffer solution [2 parts of 1.2 M sodium citrate ($Na_3C_6H_5O_7{\cdot}2H_2O$, Baker) and 1 part of 1 M sodium bicarbonate ($NaHCO_3$, Spectrum)]. The temperature was raised to ~70ºC. A reducing agent [sodium dithionite ($Na_2S_2O_4$), 100 mg, Matheson] was then added to the sample. The clay was allowed to react for ~4 h, which has been shown to be sufficient time for nearly complete reduction of nontronite (Komadel *et al.*, 1990). The extent of reduction was verified by the color of the suspension, which turned deep blue in color and then bluish gray, indicating that the majority of structural Fe had been reduced (Komadel *et al.*, 1990). The reduced sample was washed twice with N_2-sparged 18 MΩ-cm deionized water and then allowed to dry in the glovebox.

To prepare samples for Attenuated Internal Reflection Fourier Transform Infrared (ATR-FTIR) analysis, ~2 mg of clay was suspended in 1 mL of deuterated water (D_2O) which was used as the suspension medium to eliminate complication of the Si−O stretching region by the intense H_2O librational band at 686 cm^{-1} and thereby improve the quality of the baseline fits used in the spectral analysis.

ATR-FTIR spectroscopy

Infrared spectra of the nontronite suspensions were recorded using a Thermo Nicolet 3700 Fourier-transform infrared spectrometer equipped with a deuterated triglycine sulfate (DTGS) detector and *Omnic* software, version 7.2. Spectra are the average of 64 scans with a nominal resolution of 1 cm^{-1} at increment steps of 0.481 cm^{-1} from 4000 to 500 cm^{-1}. Samples were placed on a horizontal attenuated total internal reflection (ATR) apparatus (Pike Technologies) for analysis. The internal reflection element (IRE) was a horizontal 80 mm × 10 mm × 4 mm trapezoidal ZnSe crystal with a 60º angle of incidence and eight internal reflections. The IRE was mounted in a trough plate, which was used to contain the aqueous suspensions for analysis. A holographic wire polarizer (Thorlabs) was used to select the polarization of the incident radiation with the electric field oriented either parallel to the plane of incidence (p-polarized) or perpendicular to it (s-polarized). The orientation of the electric field in each polarization is shown in Figure 1.

A background spectrum with one polarization of light was first recorded with the empty sample cell in place. The clay suspension was then added to the sample cell of the ATR apparatus within the glovebox, covered with Parafilm, and then quickly transferred to the N_2-purged sample compartment of the spectrometer. The suspen-

https://doi.org/10.1346/CCMN.2009.0570209 Published online by Cambridge University Press

sion was allowed to sit for several minutes to allow the formation of a stable, oriented film on the IRE as demonstrated by Johnston and Premachandra (2001). The sample spectrum was then acquired and 'ratioed' to the background spectrum. Without disturbing the sample, a second spectrum was taken using the other polarization of light, followed by a background spectrum of the empty cell. Each sample and corresponding background was scanned with continuous purging of the spectrometer with dry N_2.

Spectral analysis

Spectral analysis of the Si–O stretching region (900–1200 cm^{-1}) was accomplished using the *Peak Fit* software package, version 4.12 (Systat). Baseline subtraction was accomplished with a linear algorithm. Peaks were fit to Voigt (Gaussian-Lorentzian) line shapes. The amplitudes, band positions, half-widths, and Gaussian/Lorentzian compositions of the individual bands were optimized. No parameters were locked for the optimization of line shapes. Values of r^2 for the fits were > 0.98.

RESULTS

The absorption spectra of a portion of the Si–O stretching region of unaltered NAu-1 obtained with both p- (a) and s-polarized (b) incident radiation are presented in Figure 2. The raw data are the circles. The solid line on top is the best fit, composed of the peaks given below each spectrum. The broad feature at ~1020 cm^{-1} can be fit to two component peaks at 1011 and 1038 cm^{-1}. Previous IR studies of nontronites (Farmer and Russell, 1964; Yan and Stucki, 2000) and of NAu-1 in particular (Frost *et al.*, 2002; Merola *et al.*, 2007), found that the Si–O stretching region is made up of two overlapping pairs of peaks at 1000–1050 and 1050–1100 cm^{-1}. The peak at 1038 cm^{-1} is the out of plane Si–O stretch (dotted line) corresponding to the apical Si–O bond, while the other three are all in-plane stretching modes. The feature in Figure 2 corresponds to the stronger pair in this region. The major difference between the spectrum obtained with p-polarized light (Figure 2a) and the s-polarized spectrum (Figure 2b), is that the out-of-plane peak is distinctly more intense in the p-polarized spectrum.

Since spectra obtained with both polarizations of incident radiation were taken using the same clay film, one may define the dichroic ratio, R_{ATR}, as follows:

$$R_{ATR} = \frac{A_S}{A_P}$$

In the case of unaltered NAu-1 as shown in Figure 2, R_{ATR} for the out-of-plane (apical) Si–O stretch is 0.2. Because the p-polarization has a vector component of the electric field perpendicular to the surface of the crystal but the s-polarization does not (see Figure 1), this low value of the dichroic ratio indicates that the apical Si–O bond (see Figure 3) responsible for the out-of-

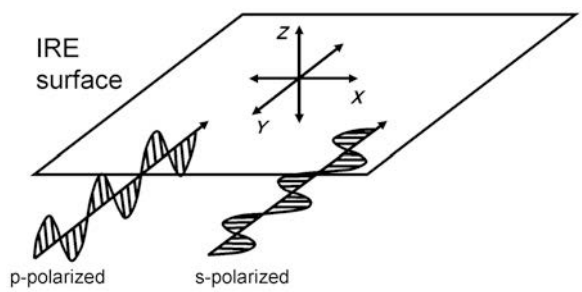

Figure 1. Schematic representation of the two polarizations of incident radiation used in ATR. The plane of the electric field in each case is shown relative to the surface of the IRE, which resides in the *x-y* plane. P-polarized radiation has a vector component of the electric field perpendicular to the IRE surface, while the electric field of s-polarized radiation lies completely in the plane of the IRE surface.

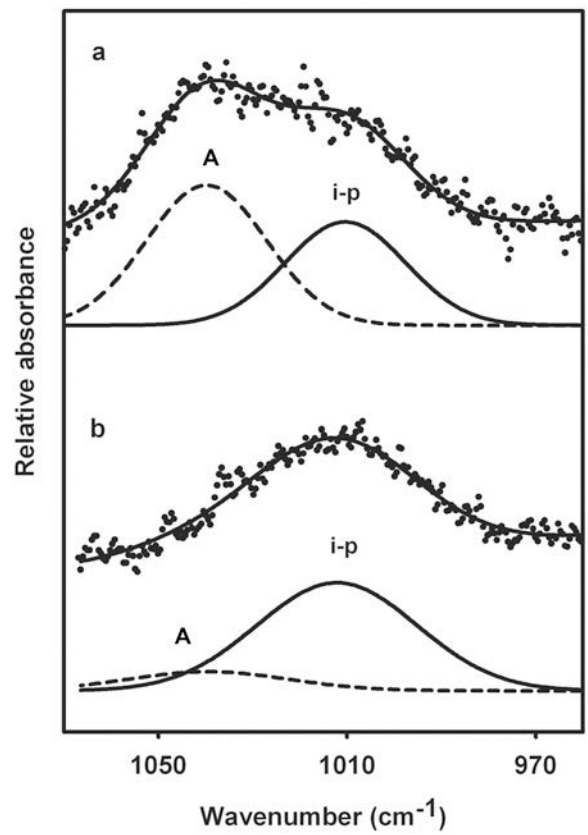

Figure 2. ATR-FTIR absorption spectra of the Si–O stretching region of unaltered NAu-1 using p-polarized (a) and s-polarized (b) incident radiation. The raw data are the circles, while the solid line on top is the best fit, composed of the peaks given below each spectrum. The labels indicate the components due to the in-plane (i-p) and out-of plane, apical (A) Si–O stretching modes.

https://doi.org/10.1346/CCMN.2009.0570209 Published online by Cambridge University Press

plane stretch is oriented almost perpendicular to the surface of the ATR crystal. This observation confirms that the basal (001) surfaces of the individual clay platelets are aligned parallel to the ATR crystal and that the clay film is indeed well oriented. This finding is in agreement with previous ATR-FTIR studies of clay suspensions, which demonstrated that clay particles in aqueous suspension form a highly oriented thin film (25–50 nm) on the surface of a ZnSe IRE with the (001) faces of the platelets parallel to the IRE surface (Johnston and Premachandra, 2001).

The absorption spectra of the Si–O stretching region of reduced NAu-1 using both p-polarized (a) and s-polarized (b) incident radiation are given in Figure 4. The apical Si–O stretch (dotted line) has shifted to a higher wavenumber, 1044 cm^{-1}, in agreement with previous studies of reduction in ferruginous smectite (Yan and Stucki, 1999). Note that while the out-of-plane peak is quite apparent in the p-polarized spectrum, it is almost non-existent in the s-polarized spectrum. Thus, R_{ATR} for the apical Si–O stretch approaches zero for reduced NAu-1. The in-plane stretch present in the unaltered spectrum has shifted to a lower wavenumber (986 cm^{-1}) and a second in-plane stretch, presumably one of the peaks from the weaker pair in the 1050–1100 cm^{-1} region, has also shifted to a lower wavenumber (1011 cm^{-1}) and increased in intensity.

The absorption spectra of the Si–O stretching region of unaltered NAu-2 obtained with p-polarized (a) and s-polarized (b) radiation and the corresponding fits to the data are shown in Figure 5. Similar to the spectra of NAu-1 and in agreement with a previous IR study of NAu-2 (Frost *et al.*, 2002), the strongest pair of peaks in the Si–O stretching region of unaltered NAu-2 resides between 1050 and 1100 cm^{-1}. The peak at 1030 cm^{-1} (dotted line) is the apical Si–O stretch. The other peak at 1014 cm^{-1} is an in-plane stretch. Comparing the peak intensities for the two polarizations, R_{ATR} for the out-of-plane Si–O stretch is calculated to be 0.55.

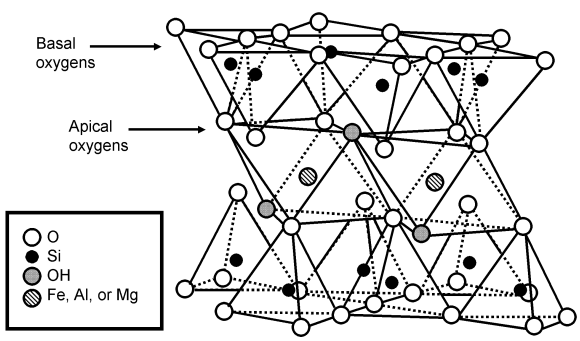

Figure 3. Structure of a nontronite, with the two tetrahedral sheets containing mostly Si and the octahedral sheet containing Fe, Al, and Mg. The apical Si–O bonds in all the tetrahedra are oriented approximately perpendicular to the basal surface of the clay.

The absorption spectra of the Si–O stretching region for reduced NAu-2 (Figure 6), compared to the spectra of unaltered NAu-2, revealed that all three in-plane Si–O stretching modes shifted to lower frequencies. The dominant in-plane peak present in the unaltered sample shifted to a lower wavenumber (990 cm^{-1}) and the two in-plane Si–O bands from the less intense pair apparently shifted from a higher wavenumber to 1008 $cm^{-1}$and 1070 cm^{-1}. In contrast, the out-of-plane apical Si–O stretch (dotted line) shifted to higher wavenumber (1050 cm^{-1}). The apical stretch is very prominent in the p-polarized spectrum (Figure 6a), but has essentially no intensity in the s-polarized spectrum (Figure 6b). In other words, R_{ATR} approaches zero.

DISCUSSION

Reduction of tetrahedral Fe^{3+}

The trends observed in the spectra of NAu-1 and NAu-2, as summarized in Table 1, are very similar. In each mineral, reduction brings about a shift in the in-plane

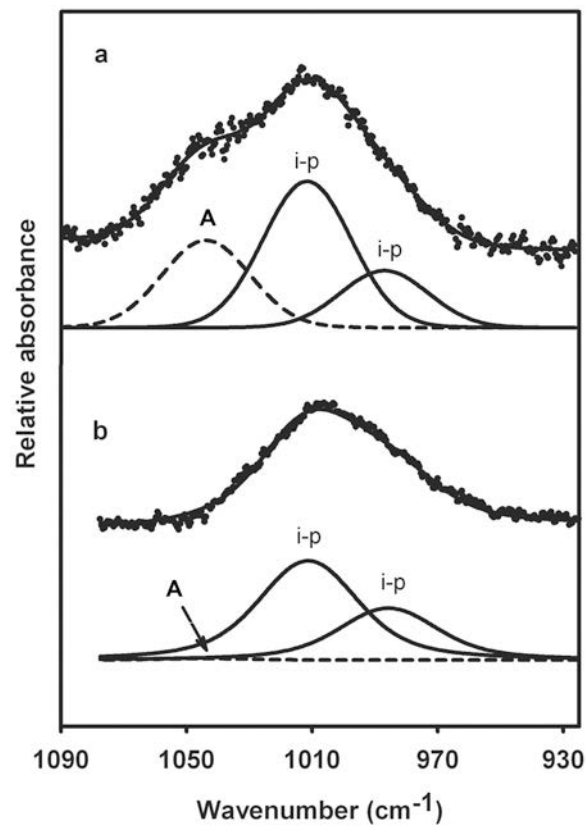

Figure 4. ATR-FTIR absorption spectra of the Si–O stretching region of reduced NAu-1 using p-polarized (a) and s-polarized (b) incident radiation. The raw data are the circles, while the solid line on top is the best fit, composed of the peaks given below each spectrum. The labels indicate the components due to the in-plane (i-p) and out-of plane, apical (A) Si–O stretching modes.

https://doi.org/10.1346/CCMN.2009.0570209 Published online by Cambridge University Press

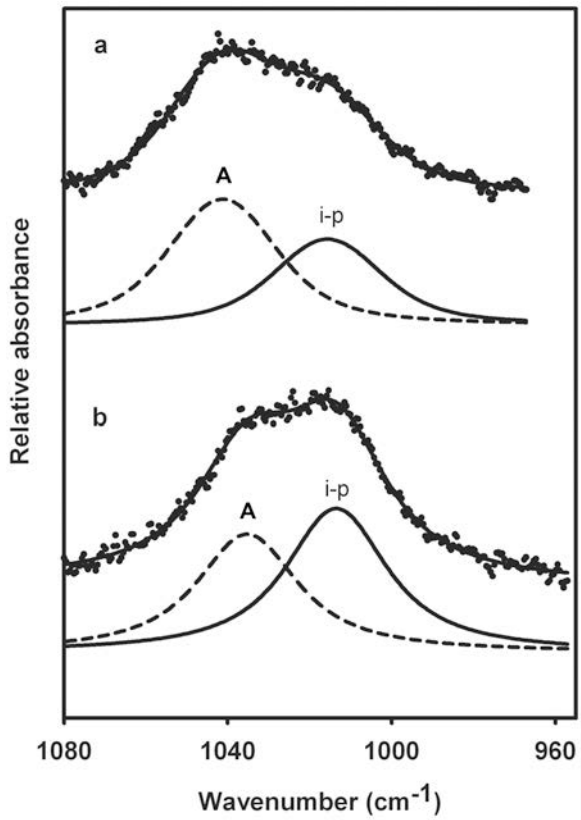

Figure 5. ATR-FTIR absorption spectra of the Si−O stretching region of unaltered NAu-2 using p-polarized (a) and s-polarized (b) incident radiation. The raw data are the circles, while the solid line on top is the best fit, composed of the peaks given below each spectrum. The labels indicate the components due to the in-plane (i-p) and out-of plane, apical (A) Si−O stretching modes.

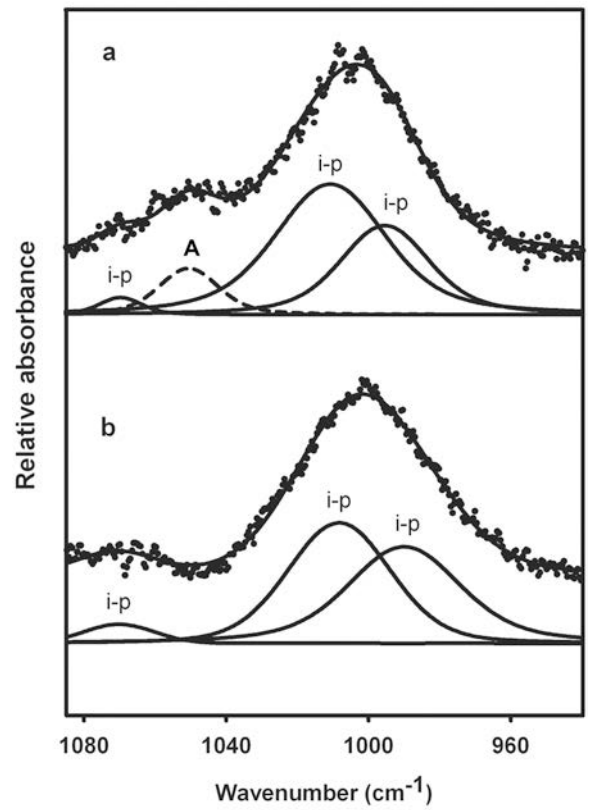

Figure 6. ATR-FTIR absorption spectra of the Si−O stretching region of reduced NAu-2 using p-polarized (a) and s-polarized (b) incident radiation. The raw data are the circles, while the solid line on top is the best fit, composed of the peaks given below each spectrum. The labels indicate the components due to the in-plane (i-p) and out-of plane, apical (A) Si−O stretching modes.

Si−O stretching modes to lower frequencies while the out-of-plane Si−O stretch shifts to higher frequency and exhibits a decrease in its dichroic ratio. Given that NAu-2 contains tetrahedral Fe^{3+} and NAu-1 does not, the similarity of the changes in their IR spectra as a result of reduction suggests that either the tetrahedral Fe^{3+} is not reduced, or the reduction of this species does not have a substantial influence on the changes which occur in the silicate structure. In the reduction of both minerals, a four-fold molar excess of sodium dithionite relative to the mineral's Fe content was used and sufficient time given to allow the nearly complete reduction of structural Fe as demonstrated by the resulting gray color of the nontronite (Komadel, *et al*., 1990). Previous studies of the microbial reduction (Jaisi *et al.*, 2005) of NAu-2 provided evidence that the tetrahedral Fe^{3+} in NAu-2 is preferentially reduced before the octahedral fraction. The tetrahedral Fe^{3+} in the NAu-2 in the current study, therefore, should be reduced.

Previous studies pointed out that the ionic radius of Fe^{2+} is too large to fit into the tetrahedral site in smectites (Cardile, 1989; Jaisi *et al.*, 2005), suggesting

Table 1. Summary of the observed band positions of the apical (out-of-plane) and in-plane Si−O stretching modes and the calculated dichroic ratio for each of the nontronites.

	Apical Si−O stretch (cm^{-1})	In-plane Si−O stretch (cm^{-1})	Dichroic ratio, R_{ATR}
Unaltered NAu-1	1038	1011	0.2
Reduced NAu-1	1044	986, 1011	0.55
Unaltered NAu-2	1030	1014	~0
Reduced NAu-2	1050	990, 1008, 1070	~0

https://doi.org/10.1346/CCMN.2009.0570209 Published online by Cambridge University Press

that reduction of tetrahedral Fe is followed by its release to solution. Jaisi *et al.* (2005) also reported that microbial reduction of Fe^{3+} in NAu-2 caused a decrease in the crystallite size of the nontronite, a change in the crystal-size distribution, and a release of Si into aqueous solution. They proposed that their results indicate a reductive dissolution mechanism. The results of the present study, however, argue against a loss of crystallinity of the silicate structure upon reduction of tetrahedral Fe. The spectra of reduced NAu-2 have well-defined peaks suggestive of a crystalline structure rather than an amorphous structure that one would expect if significant dissolution of the silicate had taken place. NAu-2, however, does exhibit a more dramatic structural change to the tetrahedral sheet upon reduction than NAu-1 does. The apical Si−O stretch in NAu-1 shifts six wavenumbers higher upon reduction of structural Fe, while the apical Si−O stretch in NAu-2 shifts 20 wavenumbers higher upon reduction. Although the general trends in NAu-2 are similar to those in NAu-1, the change in the silicate structure is clearly more significant, presumably as a result of the reduction of the tetrahedral Fe. Further work is needed to fully elucidate the reorganization of the tetrahedral sheet in NAu-2.

Effect of reduction on Si−O bond orientation

The ratio of the intensity of the out-of-plane Si−O stretching peak obtained with s-polarized incident radiation to its intensity with p-polarized radiation is an indication of the orientation of the apical Si-O bonds of the tetrahedral sheet relative to the surface of the ATR crystal. The lower the dichroic ratio, the closer the bond is to being perpendicular to the surface of the ATR crystal and consequently the plane of the clay layers. In both NAu-1 and NAu-2 the dichroic ratio decreases significantly upon reduction of the clay. In fact, the ratio approaches zero in both cases, indicating that the apical Si−O bond is oriented almost completely perpendicular to the plane of the clay. The magnitude of this change appears to be greater for NAu-2 than NAu-1, suggesting that the degree of structural rearrangement is more significant in NAu-2. However, one must be cautious in making a quantitative comparison between the two samples. The dichroic ratio depends on not only the orientation of the bond within the clay structure, but also the degree of orientation of the clay particles relative to each other and to the IRE surface. A more well oriented film also will result in a smaller dichroic ratio. The larger change in dichroic ratio resulting from reduction of NAu-2 may, therefore, partially be the result of an increase in the ordering of the film in addition to changes in the clay structure. In any case, the dichroic ratio value of nearly zero measured in both reduced nontronites indicates both that the films were well oriented and that the apical Si−O bond orientation is perpendicular to the (001) surface of the clay.

The increasingly perpendicular nature of the apical Si−O bond upon reduction has implications for understanding the structural rearrangement of the tetrahedral sheet in both NAu-1 and NAu-2. A previous study (Manceau *et al.*, 2000) employing polarized extended X-ray absorption fine structure (P-EXAFS) spectroscopy indicated that reduction of Garfield nontronite resulted in a structural modification that suppressed the corrugation of basal oxygen planes, typical of dioctahedral smectites, yielding a flat basal surface, as found in trioctahedral layer silicates (Lee and Guggenheim, 1981). This evidence for a flat basal surface, in combination with the perpendicular nature of the apical Si−O bond as determined in the current study, indicates that the O_{apical}−Si−O_{basal} bond angle remains fixed and the tetrahedra, as whole units, realign relative to the plane of the clay layer.

CONCLUSIONS

The IR spectra presented here yield substantial information about the structural evolution of nontronite upon reduction of Fe^{3+}. Nontronite with tetrahedral Fe^{3+}, *e.g.* NAu-2, retains the crystalline structure of the tetrahedral sheet, although the observed shifts of the Si−O stretching bands are larger than those observed in a nontronite without tetrahedral Fe^{3+}, such as NAu-1. Polarized ATR-FTIR spectra indicate that the apical Si−O bond changes orientation and becomes nearly perpendicular to the plane of the clay layer upon reduction. This observation is indicative of trioctahedral domain formation and suggests that the tetrahedra reorient as whole units, becoming upright relative to the (001) surface.

REFERENCES

Cardile, C.M. (1989) Tetrahedral iron in smectite: A critical comment. *Clays and Clay Minerals*, **37**, 185−188.

Cervini-Silva, J., Wu, J., Larson, R.A., and Stucki, J.W. (2000) Transformation of chloropicrin in the presence of iron-bearing clay minerals. *Environmental Science and Technology*, **34**, 915−917.

Cervini-Silva, J., Kostka, J.E., Larson, R.A., Stucki, J.W., and Wu, J. (2003) Dehydrochlorination of 1,1,1-trichloroethane and pentachloroethane by microbially reduced ferruginous smectite. *Environmental Toxicology and Chemistry*, **22**, 1046−1050.

Drits, V.A. and Manceau, A. (2000) A model for the mechanism of Fe^{3+} to Fe^{2+} reduction in dioctahedral smectites. *Clays Clay Minerals*, **48**, 185−195.

Elsner, M., Schwarzenbach, R.P., and Haderlein, S.B. (2004) Reactivity of Fe(II)-bearing minerals toward reductive transformation of organic contaminants. *Environmental Science and Technology*, **38**, 799−807.

Farmer, V.C. and Russell, J.D. (1964) The infra-red spectra of layer silicates. *Spectrochimica Acta*, **20**, 1149−1173.

Fialips, C.-I., Huo, D., Yan, L., Wu, J., and Stucki, J.W. (2002a) Infrared study of reduced and reduced-reoxidized ferruginous smectite. *Clays and Clay Minerals*, **50**, 455−469.

Fialips, C.-I., Huo, D., Yan, L., Wu, J., and Stucki, J.W.

(2002b) Effect of Fe oxidation state on the IR spectra of Garfield nontronite. *American Mineralogist*, **87**, 630–641.

Frost, R.L., Kloprogge, J.T., and Ding, Z. (2002) The Garfield and Uley nontronites – an infrared spectroscopic comparison. *Spectrochimica Acta Part A*, **58**, 1881–1894.

Gates, W.P., Slade, P.G., Manceau, A., and Lanson, B. (2002) Site occupancies by iron in nontronites. *Clays and Clay Minerals*, **50**, 223–239.

Hofstetter, T.B., Neumann, A., and Schwarzenbach, R.P. (2006) Reduction of nitroaromoatic compounds by Fe(II) species associated with iron-rich smectites. *Environmental Science and Technology*, **40**, 235–242.

Jaisi, D.P., Kukkadapu, R.K., Eberl, D.D., and Dong, H. (2005) Control of Fe(III) site occupancy on the rate and extent of microbial reduction of Fe(III) in nontronite. *Geochimica et Cosmochimica Acta*, **69**, 5429–5440.

Johnston, C.T. and Premachandra, G.S. (2001) Polarized ATR-FTIR study of smectite in aqueous suspension. *Langmuir*, **17**, 3712–3718.

Keeling, J.L., Raven, M.D., and Gates, W.P. (2000) Geology and characterization of two hydrothermal nontronites from weathered metamorphic rocks at the Uley Graphite Mine, South Australia. *Clays and Clay Minerals*, **48**, 537–548.

Kloprogge, J.T. and Frost, R.L. (2005) Infrared emission spectroscopy of clay minerals. Pp. 99–124 in: *Application of Vibrational Spectroscopy to Clay Minerals and Layered Double Hydroxides* (J.T. Kloprogge, editor). CMS Workshop Lectures, **13**, The Clay Minerals Society, Boulder, Colorado, USA.

Komadel, P., Lear, P.R., and Stucki, J.W. (1990) Reduction and reoxidation of nontronite: Extent of reduction and reaction rates. *Clays and Clay Minerals*, **38**, 203–208.

Komadel, P., Madejová, J., and Stucki, J.W. (1995) Reduction and reoxidation of nontronite: Questions of reversability. *Clays and Clay Minerals*, **43**, 105–110.

Lee, J.H. and Guggenheim, S. (1981) Single crystal X-ray refinement of pyrophyllite-1Tc. *American Mineralogist*, **66**, 350–357.

Lee, K., Kostka, J.E., and Stucki, J.W. (2006) Comparisons of structural Fe reduction in smectites by bacteria and dithionite: An infrared spectroscopic study. *Clays and Clay Minerals*, **54**, 195–208.

Madejová, J. (2003) FTIR techniques in clay mineral studies. *Vibrational Spectroscopy*, **31**, 1–10.

Manceau, A., Drits, V.A., Lanson, B., Chateigner, J., Wu, J., Huo, D., Gates, W.P., and Stucki, J.W. (2000) Oxidation-reduction mechanism of iron in dioctahedral smectites: II. Crystal chemistry of reduced Garfield nontronite. *American Mineralogist*, **85**, 153–172.

Merola, R.B., Fournier, E.D., and McGuire, M.M. (2007) Spectroscopic investigations of Fe^{2+} complexation on nontronite clay. *Langmuir*, **23**, 1223–1226.

Nzengung, V.A., Castillo, R.M., Gates, W.P. and Mills, G.L. (2001) Abiotic transformation of perchloroethylene in homogeneous dithionite solution and in suspensions of dithionite-treated clay minerals. *Environmental Science and Technology*, **35**, 2244–2251.

Ribeiro, F.R., Lee, K., Stucki, J.W., and Fabris, J.D. (2004a) Effects of redox reactions on the structure of Garfield nontronite: A Mössbauer spectroscopic study. Pp. 467–470 in: *Applied Mineralogy, Developments in Science and Technology* (M. Pecchio *et al*., editors). ICAM, Sao Paulo, Brazil.

Ribeiro, F.R., Stucki, J.W., Larson, R.A., Marley, K.A., Komadel, P., and Fabris, J.D. (2004b) Degradation of oxamyl by redox-modified smectites: Effects of pH, layer charge, and extent of Fe reduction. Pp. 471–474 in: *Applied Mineralogy, Developments in Science and Technology* (M. Pecchio, F.R.D. Andrade, L.Z D'Agostino, H. Kahn, L.M. Sant'Agostino, and M.M.M.L. Tassinari, editors). ICAM, Sao Paulo, Brazil.

Stucki, J.W. and Roth, C.B. (1976) Interpretation of infrared spectra of oxidized and reduced nontronite. *Clays and Clay Minerals*, **24**, 293–296.

Vaniman, D. (2001) *Standard operating procedure for clay mineral and zeolite separation*. Los Alamos National Laboratory, SOP-09.05.

Xu, J.C., Stucki, J.W., Wu, J., Kostka, J.E., and Sims, G.K. (2001) Fate of atrazine and alachlor in redox-treated ferruginous smectite. *Environmental Toxicology and Chemistry*, **20**, 2717–2724.

Yan, L.B. and Bailey, G.W. (2001) Sorption and abiotic redox transformation of nitrobenzene at the smectite-water interface. *Journal of Colloid and Interface Science*, **241**, 142–153.

Yan, L. and Stucki, J.W. (1999) Effects of structural Fe oxidation state on the coupling of interlayer water and structural Si-O stretching vibrations in montmorillonite. *Langmuir*, **15**, 4648–4657.

Yan, L. and Stucki, J.W. (2000) Structural perturbations in the solid-water interface of redox transformed nontronite. *Journal of Colloid and Interface Science*, **225**, 429–439.

(*Received 20 June 2008; revised 2 January 2009; Ms. 0172; A.E. J. Fabris*)